

## Supporting information

### **In-situ copper-ion catalyzed synthesis of copper containing Poly (isocyanurate-Urea) Xerogels with antibacterial activity and biocompatibility for biomedical applications**

Seethalakshmi Selvaraj<sup>a,b</sup>, Arya Ganesan<sup>c</sup>, SreyaPV<sup>b,c</sup>, Vengatesan Singaram<sup>\*b,c</sup>,

Deepak K.Pattanayak<sup>\*b,c</sup> and Naveen Chandrasekaran<sup>\*a,b</sup>

<sup>a</sup>*Electroplating Metal Finishing Division, CSIR-Central Electrochemical Research Institute, Karaikudi-630003, TamilNadu, India.*

<sup>b</sup>*Academy of Scientific and Innovative Research (AcSIR), Ghaziabad- 201002, India*

<sup>c</sup>*Process Engineering Division, CSIR-Central Electrochemical Research Institute, Karaikudi-630003, TamilNadu, India.*

\*Email: [naveenumr@gmail.com](mailto:naveenumr@gmail.com), [naveen@cecri.res.in](mailto:naveen@cecri.res.in)

#### **Experimental Section:**

##### **Materials and Methods:**

CuCl<sub>2</sub>.2H<sub>2</sub>O were purchased from Merck with a purity of 99%,N,N'Dimethyl formamide (DMF) was purchased from SRL with a purity of 99%, and acetone (HPLC grade) with a purity of ≥99.8% purchased from SRL, and Desmodur N75 was purchased from COVESTRO. Polypropylene molds (Dimensions) were purchased from Tarsons.

##### **Synthesis of Cu<sup>2+</sup>-PIU Xerogels:**

Different concentrations (1 wt.%, 3 wt.% and 5 wt.%) of CuCl<sub>2</sub>.2H<sub>2</sub>O was dissolved in 5 mL of DMF in Vial A. On the other hand, 1.04 g of Desmodur N-75 was dissolved in 5 mL of DMF in Vial B. After complete and homogenous dissolution of the materials in the respective vials. The solution were mixed together and shaken well and the resultant sol was poured in polypropylene molds (1.7cm of Diameter and height of 10 cm). The gels were found to form at ambient temperature (30°C) and pressure based on the concentration of the CuCl<sub>2</sub>.2H<sub>2</sub>O, For example, the

1 wt. % sol was found to gel within 7 minutes, whereas the 3 and 5 wt. % were found to gel within 5 and 2 minutes respectively. The wet gels were aged for 24 h at 30°C and washed with DMF (3 x 8 h) and acetone (2 x 5 h) to remove the excess unwanted precursors. The wet gels were dried under ambient pressure and temperature to yield copper ion containing polyisocyanurate-urea (Cu-PIU) gels. Figure S1 Illustrates the synthesis scheme of Cu<sup>2+</sup>-PIU xerogels. The synthetic protocol for the preparation of all Xerogels is elaborately explained in the experimental section. Figure S2 (a), (b) displays the digital images of Cu<sup>2+</sup>-PIU wet gels and Xerogels.

### **Physical and Chemical Characterization:**

X-ray diffraction (XRD) patterns for all the samples were recorded using a Bruker D8 Advance X-ray diffractometer with a Cu K $\alpha$  radiation ( $\lambda = 1.5418 \text{ \AA}$ ). FT-IR analysis for all the samples was carried out using a Bruker Tensor 27 (Optik GmbH) using an RT DLaTGS (Varian) detector. Thermogravimetric analysis (TGA) was performed on the synthesized materials using a TGA/SDT Q600 from TA Instruments, USA at a scanning rate of 5 °C/min, from room temperature (30 °C) to 800 °C under air conditions. X-ray photoelectron spectroscopy (XPS) was performed using SPECS with a Phoibos 100 MCD analyzer with a pass energy of 20 eV (Al K $\alpha$  anode (1486.6 eV)) under ultrahigh vacuum ( $5 \times 10^{-10}$  mbar). Morphological characterizations were performed using a Field emission scanning electron microscope (FESEM, Zeiss Supra 55VP), and High-resolution transmission electron microscope (HR-TEM) images for all the samples were taken using a Tecnai G2 (FEI).

### **Antibacterial Study.**

Successfully synthesized polyisocyanurate urea (PIU) gels are subjected to antibacterial property evaluation in both gram positive '*Staphylococcus aureus*' and gram negative '*Escherichia coli*'

strains of bacteria. The bacterial culture was purchased from MTCC Chandigarh, as lyophilized cells transferred into nutrient broth and incubated at 37 °C for 24 hrs. Antibacterial activity of PIU samples incorporated with copper was analyzed using zone of inhibition method. Bacterial solution of 10<sup>4</sup> CFU/mL was prepared, and 100 µL from the bacterial solution was streaked over the agar plate to incubate 1, 3, 5 wt. % of copper loaded samples. An antibiotic soaked disc (Penicillin and Streptomycin 100X) was used as positive control while neat PUA was used as negative control over the culture plate and stored at 37 °C for 24 hrs. After the incubation period antibacterial activity of each samples condition was analyzed by measuring the zone formed around the samples.

### **Cytocompatibility study**

*In-vitro* biocompatibility study was carried out to understand the biocompatibility of the material. Here the Cytotoxicity study was tested against human osteoblast like cells MG63 purchased from NCCS, Pune. The cells were sub-cultured in a medium of Dulbecco's modified Eagle's medium (DMEM), fetal bovine serum (FBS), Penicillin-Streptomycin in defined concentration and 10000 cells were seeded along with samples in the 96 well plate. The samples along with cells were grown in a CO<sub>2</sub> incubator at 37 °C with 5% CO<sub>2</sub> for 2 and 3 day evaluation. After the incubation period medium was replaced to evaluate the cell viability over samples using thiazolyl blue tetrazoliumbromide (Vybrant® MTT Cell Proliferation Assay Kit). MTT reagent is added over the surface of samples to analyse formazan crystals formation which indicate purple color for viable cells and incubated in CO<sub>2</sub> incubator for 3 h. 100µl Dimethyl sulfoxide (DMSO) was added to measure the absorbance of each sample at 570 nm using an ELISA reader.

## Table of contents

**Figure S1.** Schematic representation of the synthesis of Cu<sup>2+</sup>-PIU Xerogels.

**Figure S2.** Digital images of (a) Cu<sup>2+</sup>-PIU wet gels and (b) Xerogels prepared with different concentrations of CuCl<sub>2</sub>·2H<sub>2</sub>O.

**Figure S3.** XPS of High resolution (a-c) N1s, C1s, O1s spectra of PUA sample.

**Figure S4.** XPS of High resolution (a-e) N1s, C1s, O1s, Cu2p, Cl2p spectra of 1-Cu<sup>2+</sup>-PIU sample.

**Figure S5.** XPS of High resolution (a-e) N1s, C1s, O1s, Cu2p, Cl2p spectra of 3-Cu<sup>2+</sup>-PIU sample.

**Figure S6.** XPS of High resolution (a-e) N1s, C1s, O1s, Cu2p, Cl2p spectra of 5-Cu<sup>2+</sup>-PIU sample.

**Figure S7.** XRD patterns of neat PUA gel, CuCl<sub>2</sub>·2H<sub>2</sub>O, and dried gels of Cu<sup>2+</sup>-PIU Xerogels with different Cu<sup>2+</sup> ions concentrations (1, 3 and 5 wt. %).

**Figure S8.** TGA of PUA and Cu<sup>2+</sup>-PIU Xerogels with different Cu<sup>2+</sup> ions concentrations (1, 3 and 5 wt. %).

**Figure S9.** (a-d) FE-SEM-EDX of neat PUA and different Cu<sup>2+</sup> ions concentrations (1, 3 and 5 wt. %).

**Figure S10.** (a-c) FE-SEM-Particle size histogram of different Cu<sup>2+</sup> ions concentrations (1, 3 and 5 wt. %).

**Figure S11.** (a) HR-TEM image (b) Particle size distribution Histogram (c) HAADF image, (d)-(h) Elemental mapping of N, C, O, Cu, and Cl respectively of 1-Cu<sup>2+</sup>-PIU.

**Figure S12.** (a) HR-TEM image (b) Particle size distribution Histogram (c) HAADF image, (d)-(h) Elemental mapping of N, C, O, Cu, and Cl respectively of 3-Cu<sup>2+</sup>-PIU.

**Figure S13.** (a) HR-TEM image (b) Particle size distribution Histogram (c) HAADF image, (d)-(h) Elemental mapping of N, C, O, Cu, and Cl respectively of 5-Cu<sup>2+</sup>-PIU.

**Figure S14.** Cytotoxicity of control, neat PUA and Cu<sup>2+</sup> different concentrations (1, 3, 5 wt. %) observed at 48hr and 72 hr.

**Table S1.** Elemental composition of the neat PUA, and the Cu<sup>2+</sup>-PIU Xerogels with different Cu<sup>2+</sup> ions concentrations (1, 3 and 5 wt. %).

**Table S2.** XPS Binding energy of C1s, O1s, N1s, Cu2p and Cl2p.

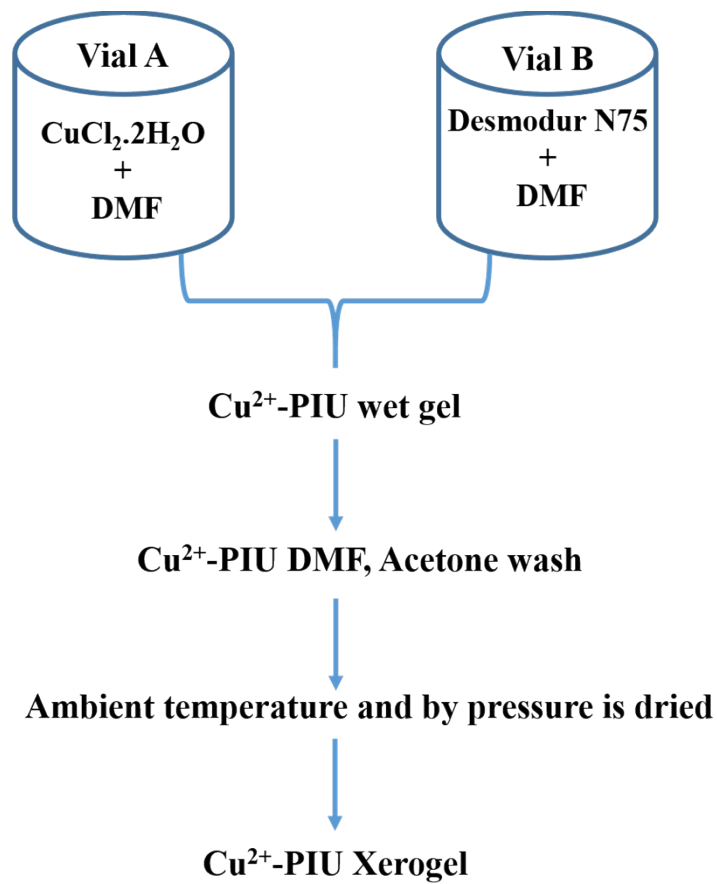


**Figure S1. Schematic representation of the synthesis of Cu<sup>2+</sup>-PIU Xerogels.**

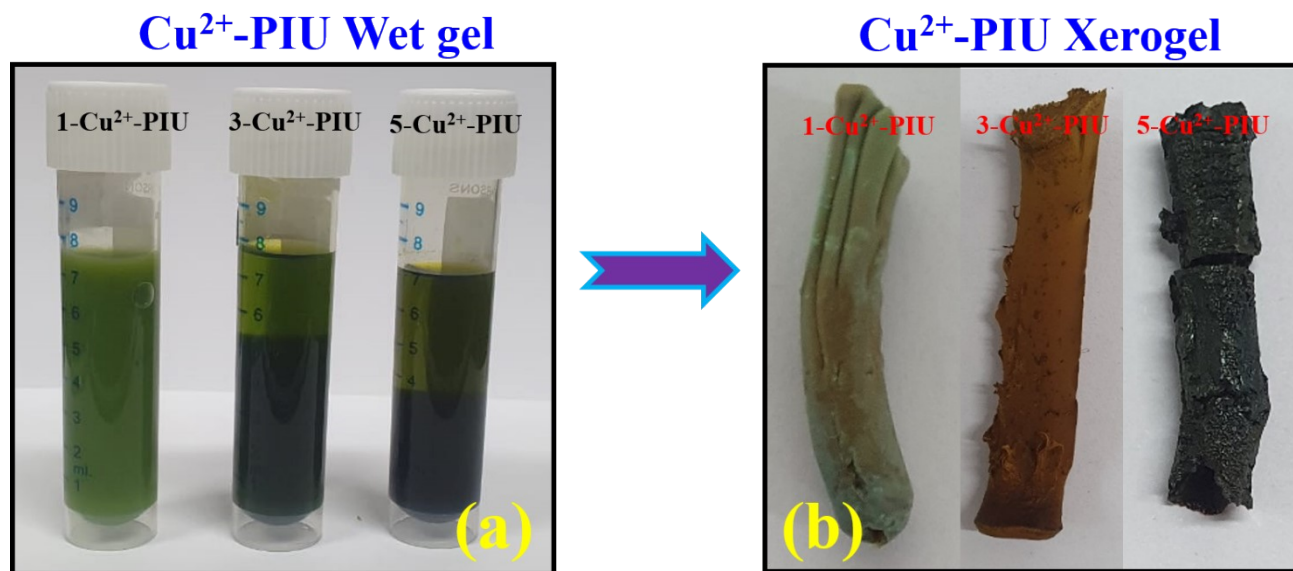


**Figure S2. Digital images of (a) Cu<sup>2+</sup>-PIU wet gels and (b) Xerogels prepared with different concentrations of CuCl<sub>2</sub>·2H<sub>2</sub>O.**

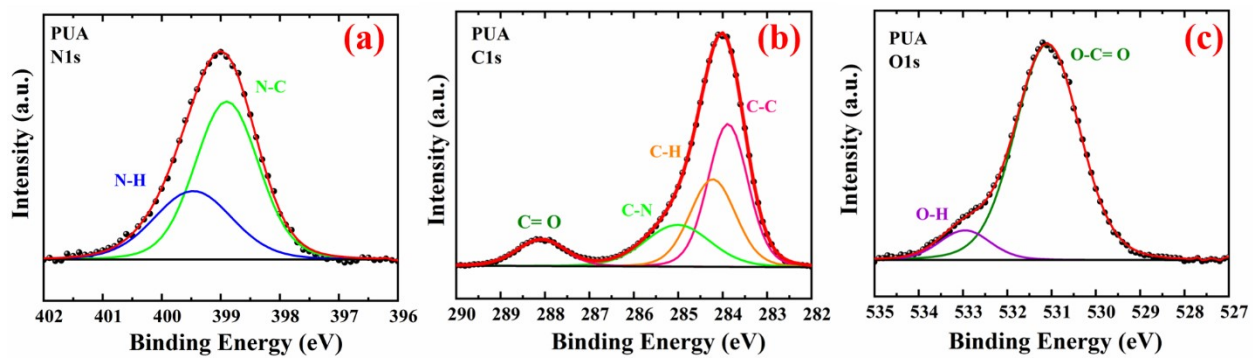


Figure S3. XPS high resolution (a-c) N1s, C1s, O1s spectra of PUA sample.



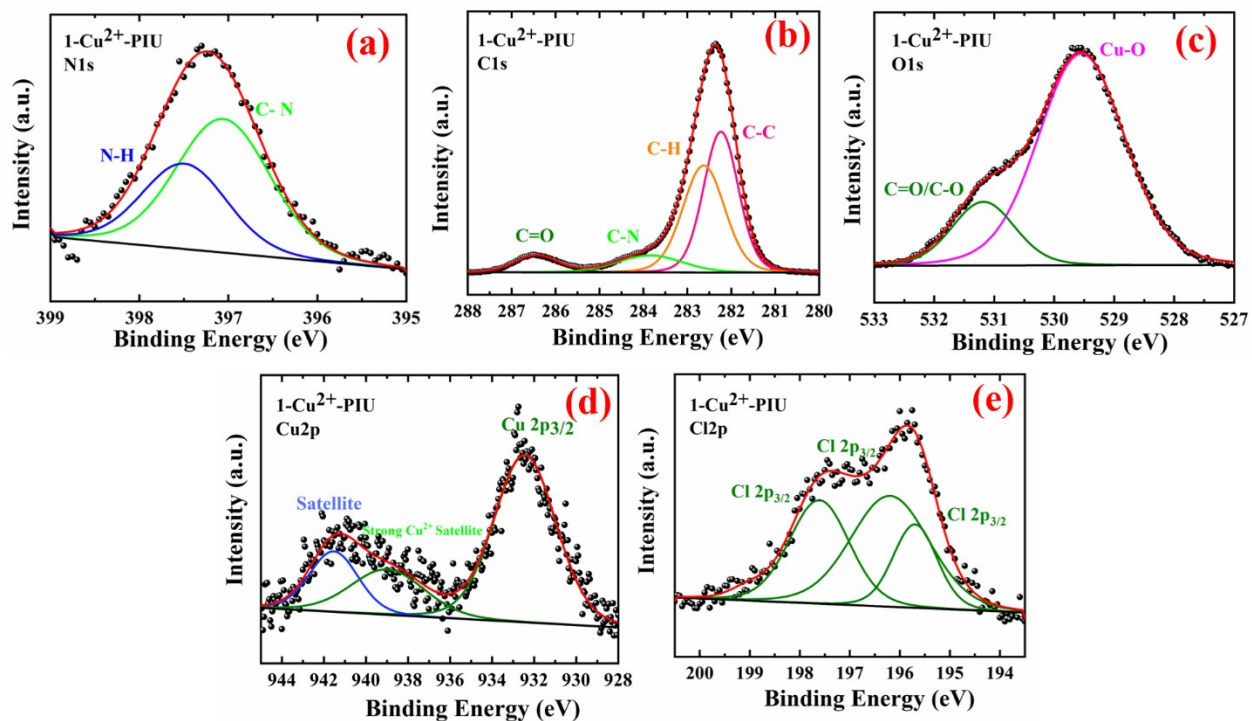


Figure S4. XPS high resolution (a-e) N1s, C1s, O1s, Cu2p, Cl2p spectra of 1-Cu<sup>2+</sup>-PIU sample.

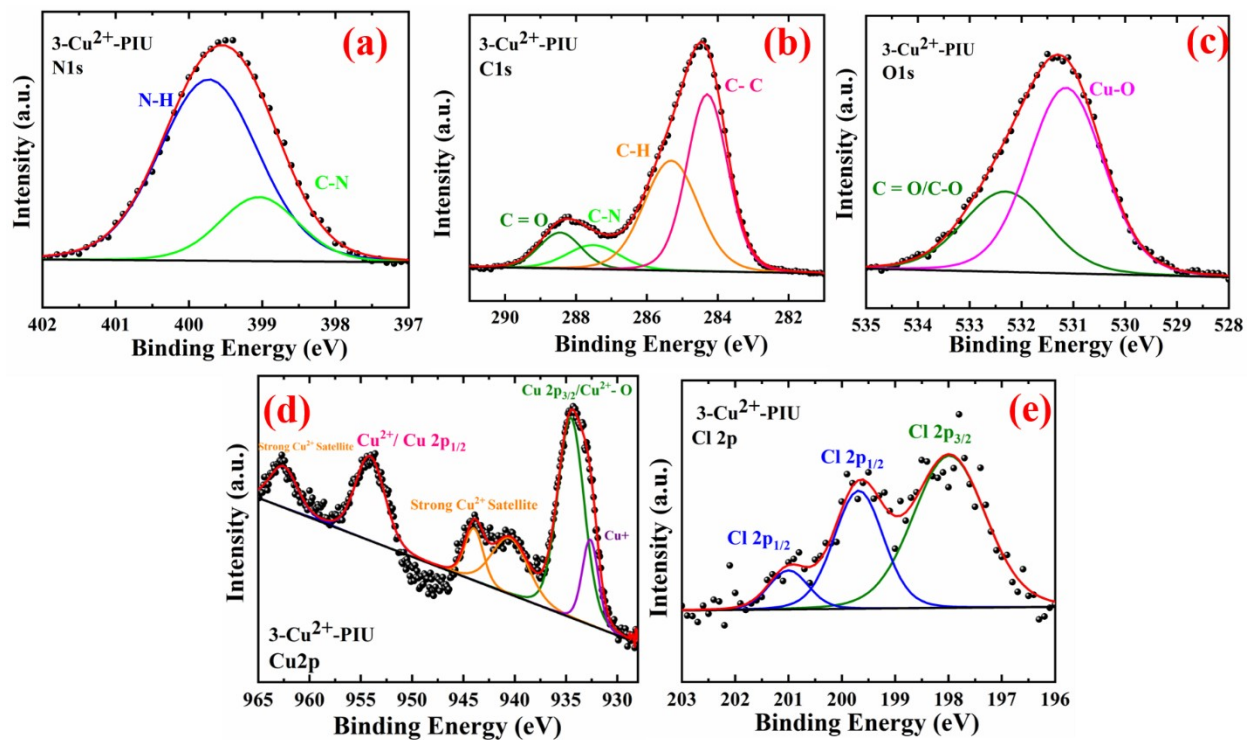


Figure S5. XPS high resolution(a-e) N1s, C1s, O1s, Cu2p, Cl2p spectra of 3-Cu<sup>2+</sup>-PIU sample.

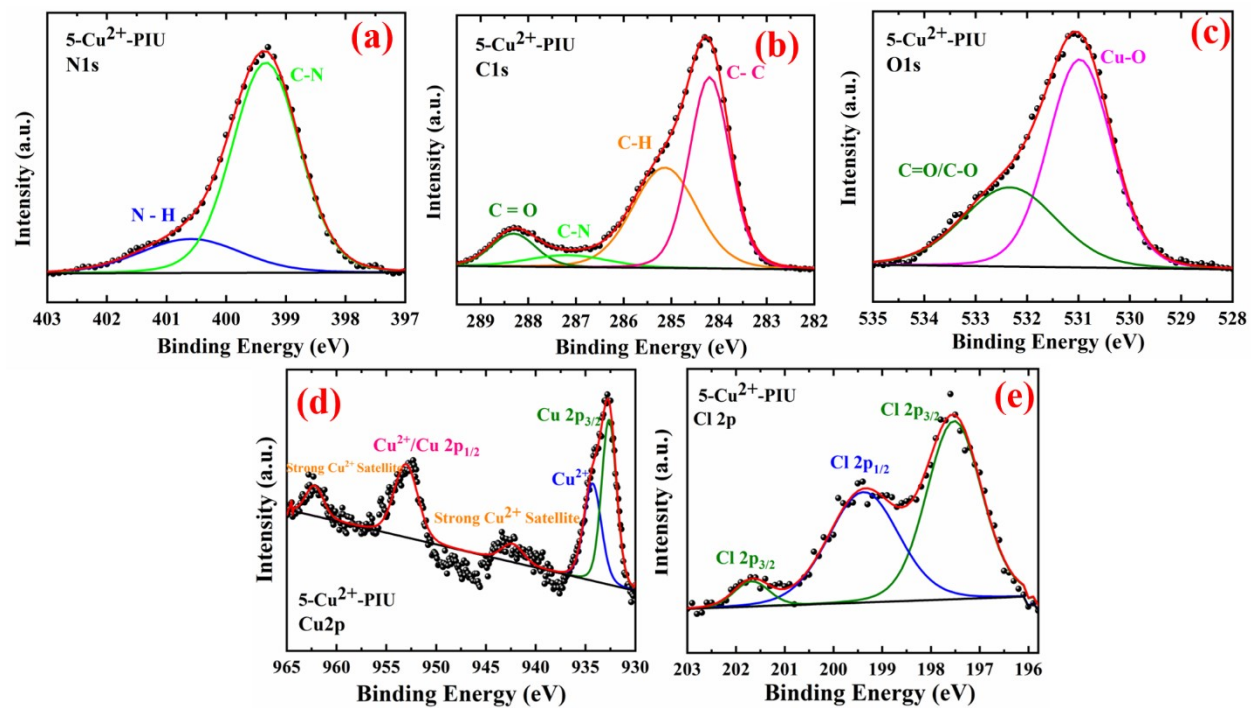


Figure S6. XPS high resolution (a-e) N1s, C1s, O1s, Cu2p, Cl2p spectra of 5-Cu<sup>2+</sup>-PIU sample.

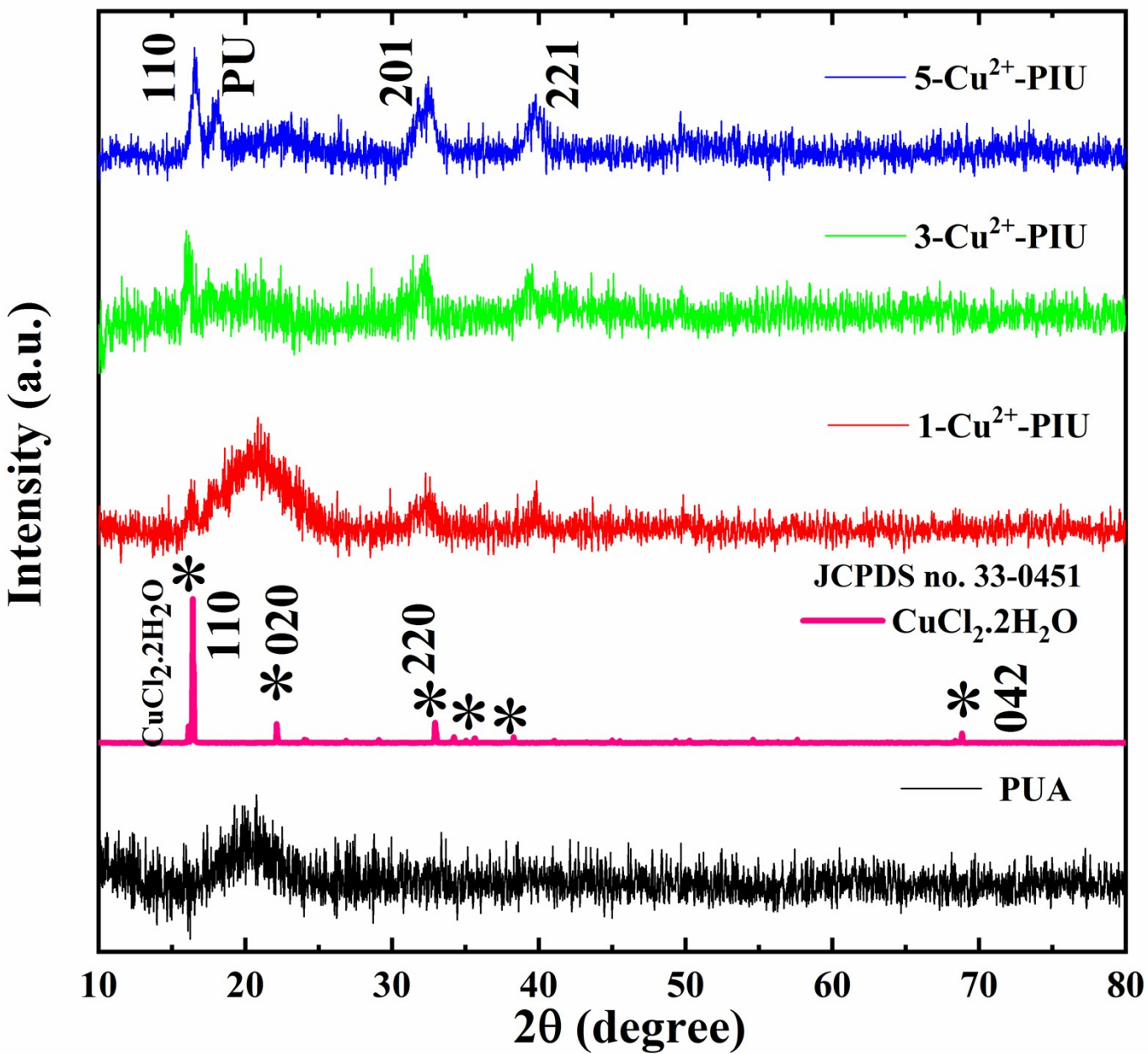


Figure S7. XRD patterns of neat PUA gel,  $\text{CuCl}_2 \cdot 2\text{H}_2\text{O}$ , and dried gels of  $\text{Cu}^{2+}$ -PIU Xerogels with different  $\text{Cu}^{2+}$  ions concentrations (1, 3 and 5 wt. %).

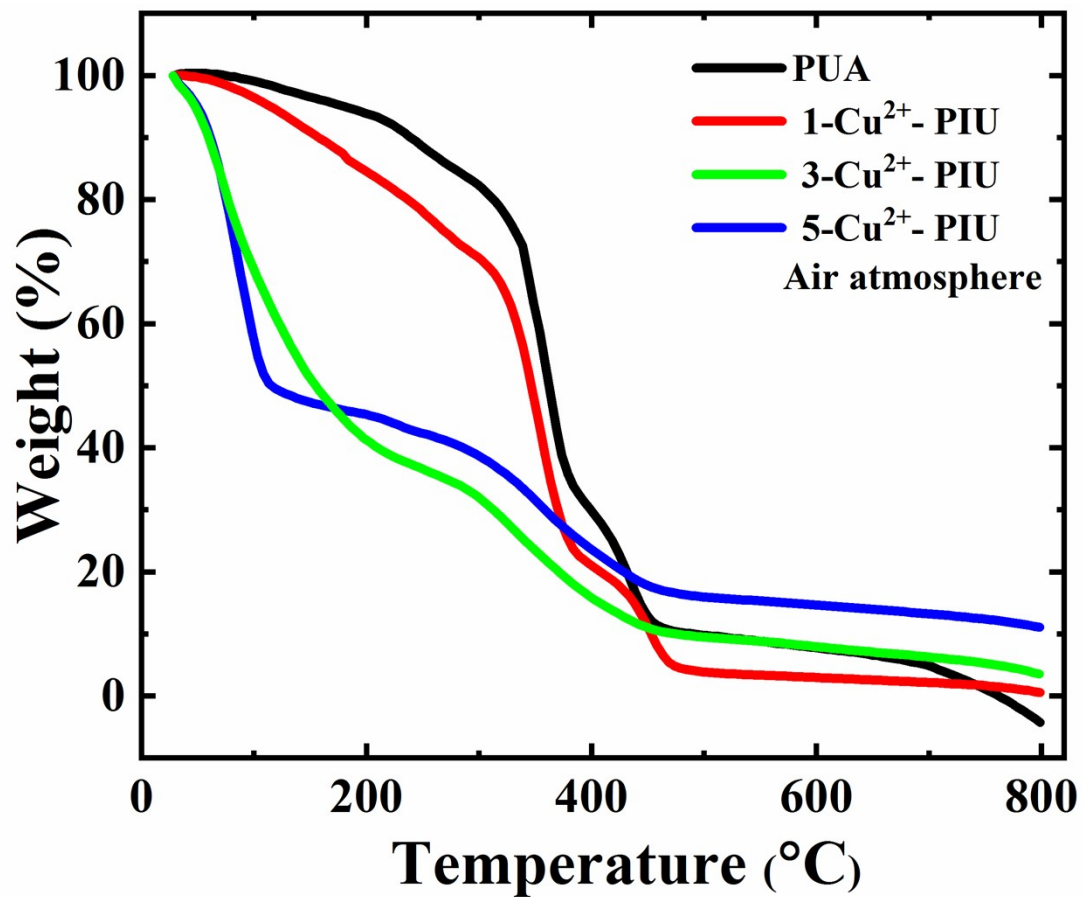
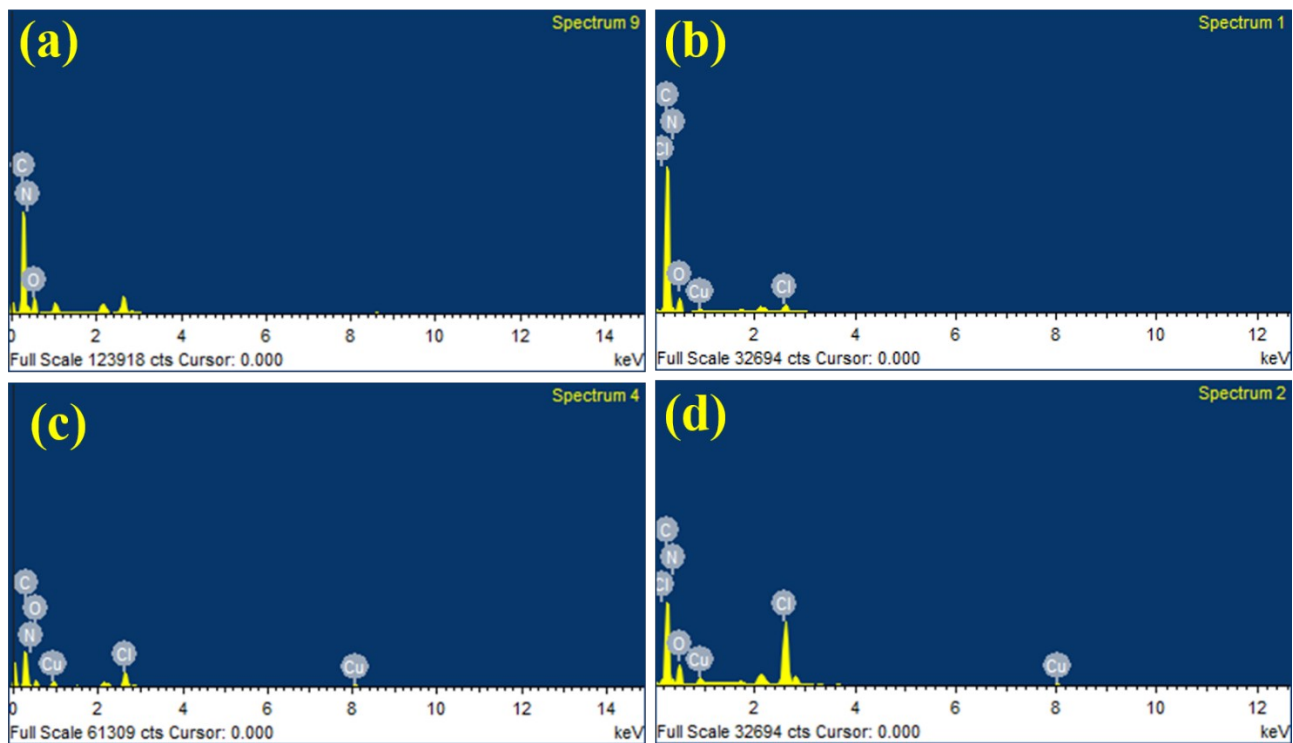
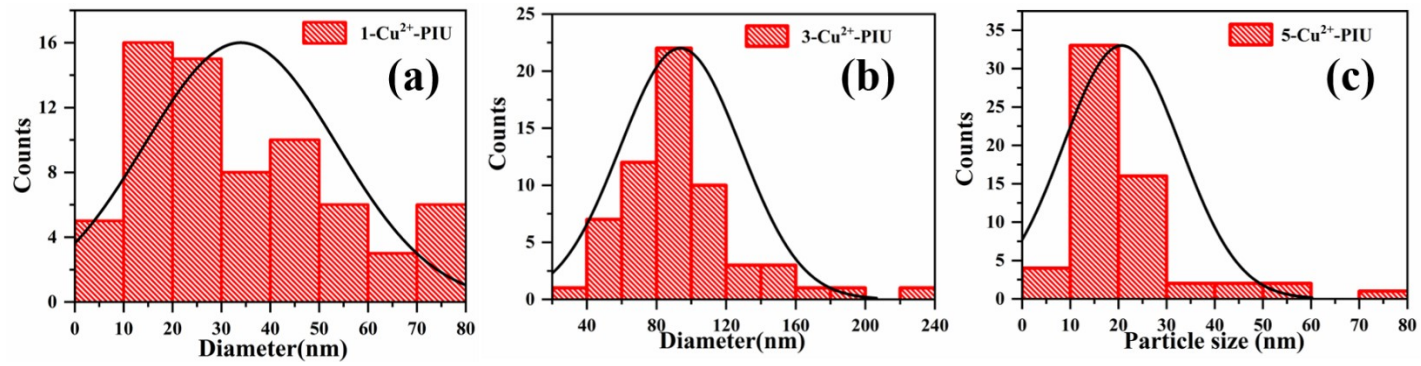


Figure S8. TGA of PUA and Cu<sup>2+</sup>-PIU Xerogels with different Cu<sup>2+</sup> ions concentrations (1, 3 and 5 wt. %).



**Figure S9. (a-d) FE-SEM-EDX of neat PUA and different  $\text{Cu}^{2+}$  ions concentrations (1, 3 and 5 wt. %).**



**Figure S10. (a-c) FE-SEM-Particle size distribution histograms of different Cu<sup>2+</sup> ion concentrations (1, 3 and 5 wt. %).**

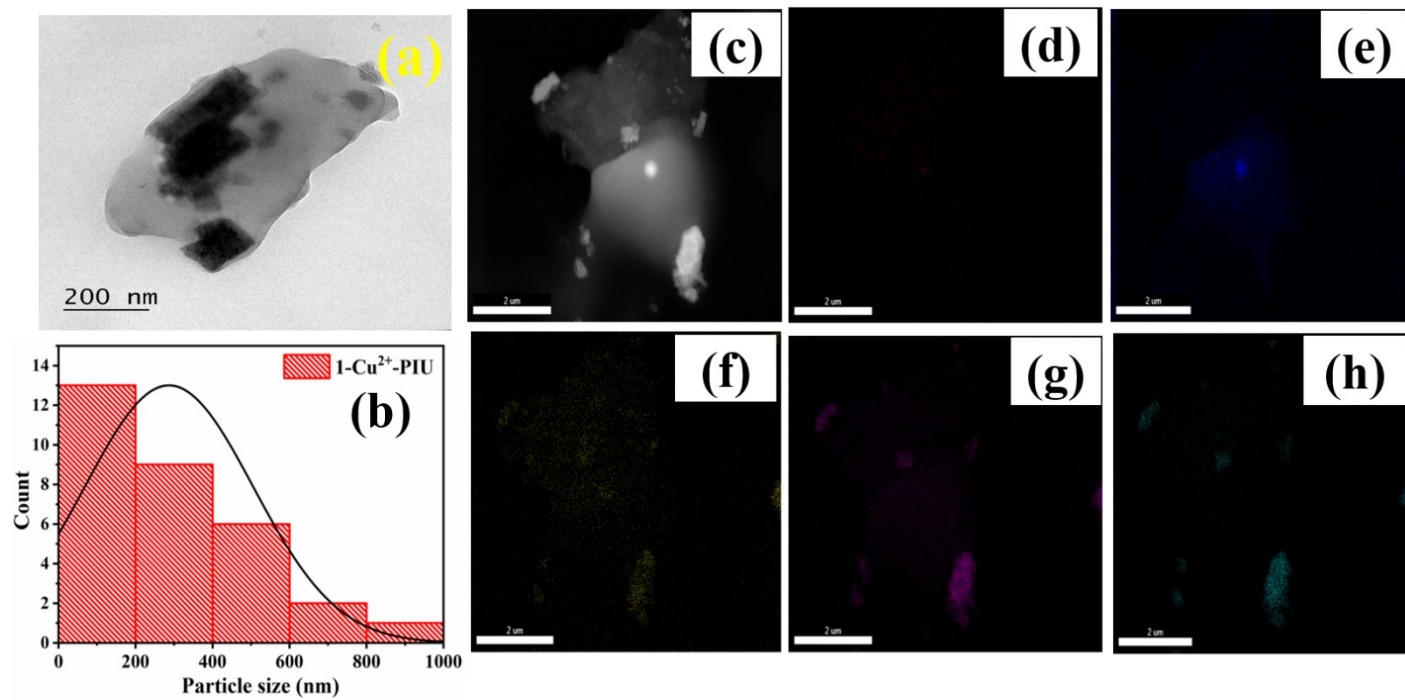


**Figure S11. (a) HR-TEM image (b) Particle size distribution Histogram (c) HAADF image, (d)-(h) Elemental mapping of N, C, O, Cu, and Cl respectively of 1-Cu<sup>2+</sup>-PIU.**



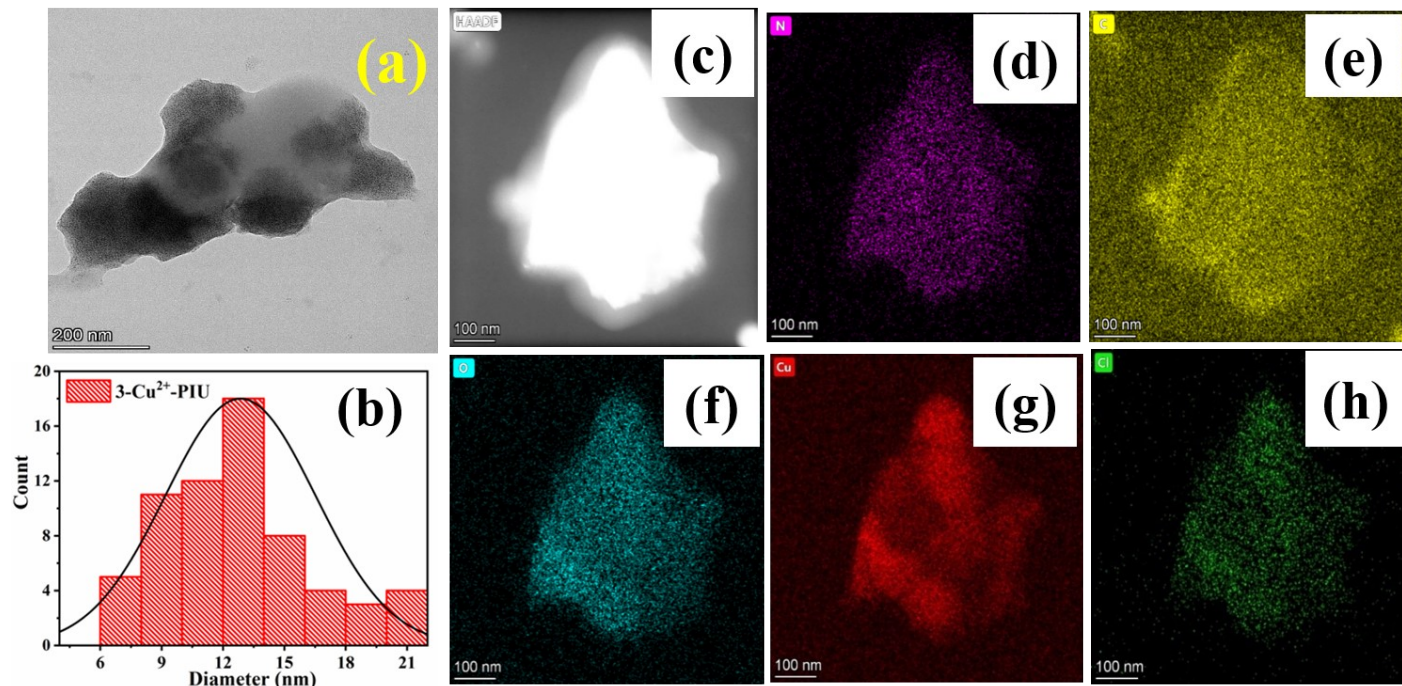


**Figure S12. (a) HR-TEM image (b) Particle size distribution Histogram (c) HAADF image, (d)-(h) Elemental mapping of N, C, O, Cu, and Cl respectively of 3-Cu<sup>2+</sup>-PIU.**

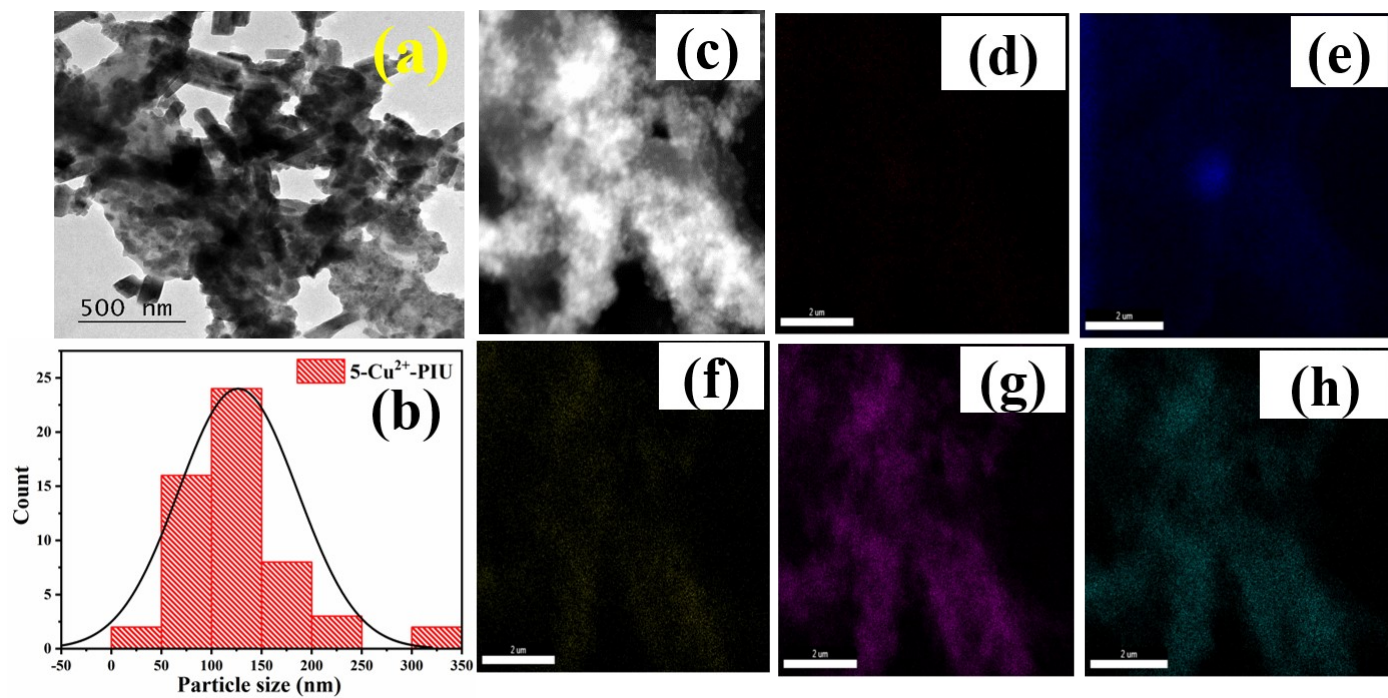


**Figure S13. (a) HR-TEM image (b) Particle size distribution Histogram (c) HAADF image, (d)-(h) Elemental mapping of N, C, O, Cu, and Cl respectively of 5-Cu<sup>2+</sup>-PIU.**

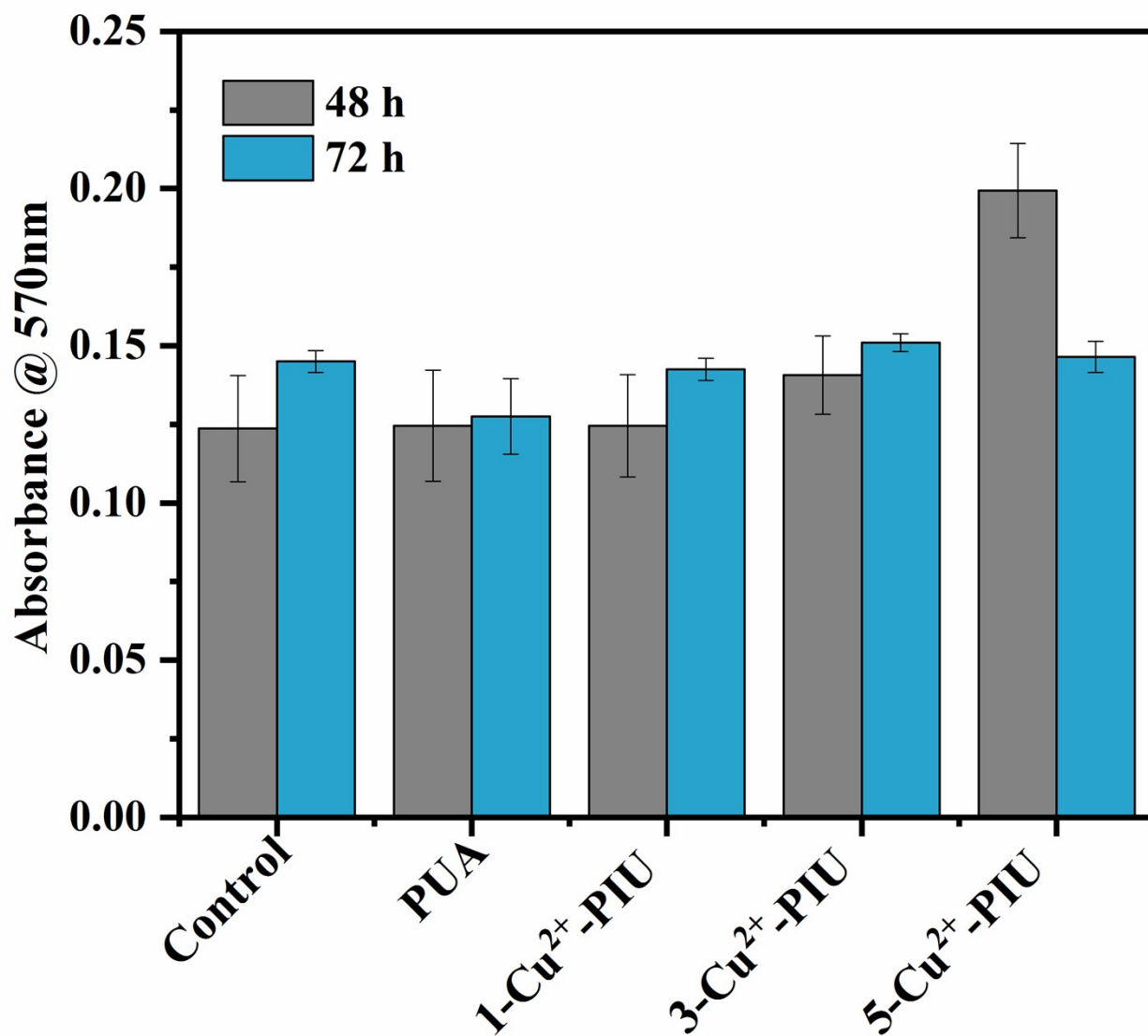


Figure S14. Cytotoxicity of control, neat PUA and Cu<sup>2+</sup> different concentrations (1, 3, 5 wt. %) observed at 48 and 72 hr.

**Table S1. Elemental composition of the neat PUA, and the Cu<sup>2+</sup>-PIU Xerogels with different Cu<sup>2+</sup> ions concentrations (1, 3 and 5 wt. %).**

<b>Element</b>	<b>PUA</b>	<b>1-Cu<sup>2+</sup>-PIU</b>	<b>3-Cu<sup>2+</sup>-PIU</b>	<b>5-Cu<sup>2+</sup>-PIU</b>
<b>N</b>	24.97	13.96	15.85	15.61
<b>C</b>	54.31	70.81	66.86	65.83
<b>O</b>	20.72	14.53	14.57	15.40
<b>Cu</b>	-	0.23	0.65	1.21
<b>Cl</b>	-	0.47	2.06	1.95

**Table S2. XPS Binding energy values from C1s, O1s, N1s, Cu2p and Cl2p high resolution spectra.**

<b>Sample Name</b>	<b>B.E. (eV) C1s</b>	<b>B.E. (eV) O1s</b>	<b>B.E. (eV) N1s</b>	<b>B.E. (eV) Cu2p</b>	<b>B.E. (eV) Cl2p</b>
<b>PUA</b>	288.1 (C=O)	532.9 (O-H)	399.47 (N-H)	-	-
	285.0 (C-N)	531.1 (O-C=O)	398.90 (N-C)	-	-
	284.2 (C-H)	-	-	-	-
	283.8 (C-C)	-	-	-	-
<b>1-Cu<sup>2+</sup>-PIU</b>	286.7 (C=O)	531.1 (C=O)/(C-O)	397.5 (N-H)	932.4 (Cu2p <sub>3/2</sub> )	197.6 (Cl2p <sub>3/2</sub> )
	283.9 (C-N)	529.5 (Cu-O)	397.0 (C-N)	-	196.1 (Cl2p <sub>3/2</sub> )
	282.6 (C-H)				
	282.2 (C-C)	-	-	-	195.7 (Cl2p <sub>3/2</sub> )
<b>3-Cu<sup>2+</sup>-PIU</b>	288.4 (C=O)	532.3 (C=O)/(C-O)	399.7 (N-H)	954.2 (Cu <sup>2+</sup> /Cu2p <sub>1/2</sub> )	201.0 (Cl2p <sub>1/2</sub> )
	287.4 (C-N)	531.1 (Cu-O)	399.04 (C-N)	934.5 (Cu2p <sub>3/2</sub> /Cu <sup>2+</sup> -O)	199.7 (Cl2p <sub>1/2</sub> )
	285.3 (C-H)	-	-	932.7 (Cu <sup>+</sup> )	197.53 (Cl2p <sub>3/2</sub> )
	284.3 (C-C)	-	-	-	-
<b>5-Cu<sup>2+</sup>-PIU</b>	288.2 (C=O)	532.39 (C=O)/(C-O)	400.64 (N-H)	952.93 (Cu <sup>2+</sup> /Cu2p <sub>1/2</sub> )	201.69 (Cl2p <sub>3/2</sub> )
	287.1 (C-N)	530.98 (Cu-O)	399.3 (C-N)	934.3 (Cu <sup>2+</sup> )	199.3 (Cl2p <sub>1/2</sub> )
	285.1 (C-H)	-	-	932.70 (Cu2p <sub>3/2</sub> )	197.54 (Cl2p <sub>3/2</sub> )
	284.1 (C-C)	-	-	-	-